

EMPIRICAL HYSTERETIC ENVELOPES FOR RC COLUMNS UNDER COMBINED CYCLIC BENDING AND TORSION

Paiboon TIRASIT¹ and Kazuhiko KAWASHIMA²

¹Graduate Student, Department of Civil Engineering, Tokyo Institute of Technology, paiboon@cv.titech.ac.jp

²Professor, Department of Civil Engineering, Tokyo Institute of Technology, kawasima@cv.titech.ac.jp
2-12-1 O-okayama Meguro-ku, Tokyo 152-8550

1. INTRODUCTION

Recently, several urban areas have dealt with the problem about the space limitation for the transportation system. One feasible solution is to employ the bridges with specific configurations such as C-bent column bridges, skewed bridges, curved bridge, etc. During an earthquake, it is obvious that bridge piers are subjected to the combined action of biaxial bending, shear and axial force. However, in the piers of such special bridges mentioned above, seismic torsion possibly occurs with other internal forces due to their irregular structural placement. This can result in the complex flexural and shear failure of these piers.

In accordance with the previous experimental researches, Hsu et al.¹ and Hsu et al.² carried out the tests on the effect of combined cyclic bending and constant torsion on the performance of composite columns with several steel sections. They revealed that the flexural capacity and ductility of composite columns decreased when a constant torsion was simultaneously applied. The effect of torsion on the deterioration of flexural strength was more considerable in the composite columns with larger aspect ratio. Kawashima et al.³ and Nagata et al.⁴ conducted a cyclic bilateral loading test and a hybrid loading test on the reinforced concrete C-bent columns, respectively. They found that the damage extremely occurred on the eccentric compression side and the residual displacement took place in this direction. This was resulted from the eccentricity of vertical axial load coupled with the bending moment and torsion from the eccentric lateral force. Otsuka et al.⁵ conducted an experimental examination on

the combined cyclic bending and torsion on the behavior of reinforced concrete columns. Their results showed that the flexural strength, the ductility and the degree of energy dissipation of columns obviously reduced as the degree of applied torsion increased. The spacing of tie reinforcement remarkably affected the torsional hysteretic loops but less significantly influenced the flexural hysteretic loops.

Nevertheless, the knowledge about the interaction between the bending moment and torsion is still limited. The behavior of columns under combined cyclic bending and torsion has not been well understood. To clarify the effect of nonlinear hysteresis torsion in RC bridge piers during an earthquake, a reliable hysteretic model is required. The model shall be verified by the experimental results. Two empirical hysteretic envelopes for flexural and torsional modes based on the authors' experimental study⁶ are proposed in this paper to serve as the basis of the hysteretic model.

2. EXPERIMENTAL PROGRAM

The authors' experimental study⁶ is briefly reviewed here to provide the basic information for the reader.

(1) Specimen Properties

Seven reinforced concrete columns with the structural properties as shown in Fig. 1 were fabricated. The columns had a 400 mm x 400 mm square cross section and They were 1750 mm tall with a 1350 mm effective height. All columns were designed based on the Japanese 1996 Design Specifications of Highway Bridges⁷. Type I

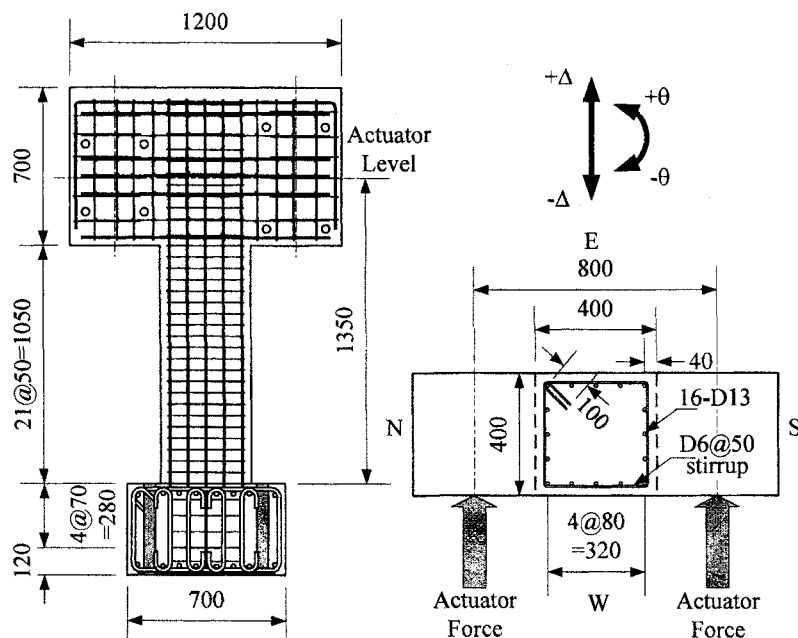


Fig. 1 Specimen configuration

Table 1 Experimental cases

Column	f'_c (MPa)	Loading scheme	r
P1	28.6	M+P	0
P2	28.3	T	∞
P3	28.4	T+P	∞
P4	32.2	T+M+P	0.5
P5	28.4	T+M+P	1
P6	32.8	T+M+P	2
P7	33.1	T+M+P	4

T: Cyclic torsion

M: Cyclic uniaxial bending

P: 160kN constant axial compression force

(middle-field) and Type II (near-field) ground motions with the moderate soil condition were assumed. The axial compressive stress at the plastic hinge region of the column due to the dead weight of superstructure was assumed to be 1 MPa. The design concrete compressive strength was 30 MPa. Sixteen 13 mm diameter deformed bars with 295 MPa nominal strength (SD295A) were provided as the longitudinal reinforcement. The same grade 6 mm diameter deformed bars were also provided as the stirrups with 50 mm spacing. The longitudinal reinforcement ratio and the tie volumetric ratio were 1.27% and 0.75%, respectively. Table 1 shows the concrete strength f'_c obtained from the cylinder test of all columns.

(2) Loadings

A series of cyclic load tests was conducted by

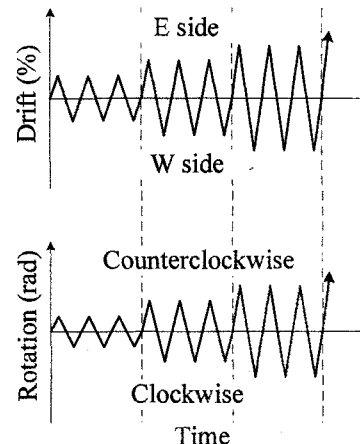


Fig. 2 Loading scheme

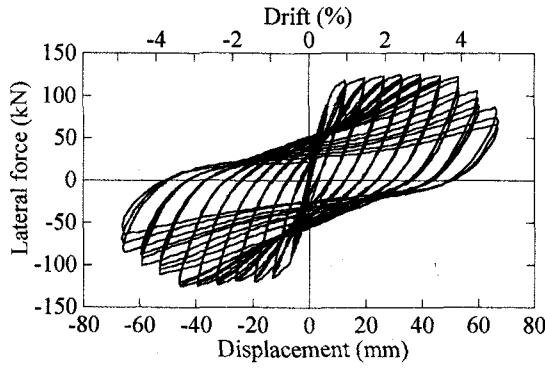
using the dynamic testing facility in Tokyo Institute of Technology. Table 1 presents the loading conditions of all columns. A constant 160 kN compression was applied to the specimens to produce the 1 MPa compressive stress in the plastic hinge region, except columns P2. The test was conducted under lateral displacement and rotation being controlled. As shown in Fig. 1, cyclic uniaxial bending was created by driving two horizontal actuators with the same displacement command while cyclic torsion and combined cyclic bending and torsion were generated by imposing different displacement commands in the two actuators. Column P1 was tested under cyclic uniaxial bending. The effect of axial force on the torsional hysteresis was inspected on columns P2 and P3. Columns P4 to P7 were tested under several combinations of cyclic bending and cyclic torsion. The rotation-drift ratio r is defined here to control the level of combined bending and torsion as

$$r = \frac{\theta}{\Delta} \quad (1)$$

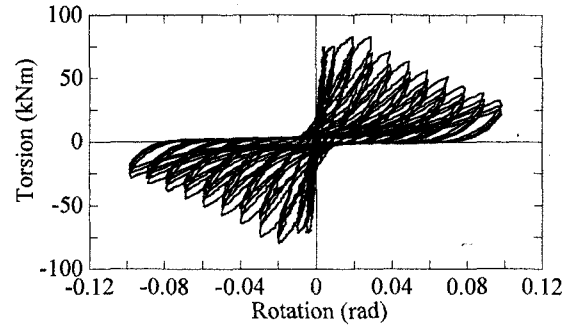
in which θ is the rotation in radian and Δ is the lateral drift at the effective height of column. The levels of combined bending and torsion of columns are presents in Table 1. Fig. 2 shows the loading pattern. Rotation and lateral displacement were applied simultaneously and each loading step was repeated 3 times.

(3) Experimental result

Fig. 3 shows the hysteresses of P1 and P3 under cyclic uniaxial bending and cyclic torsion with an

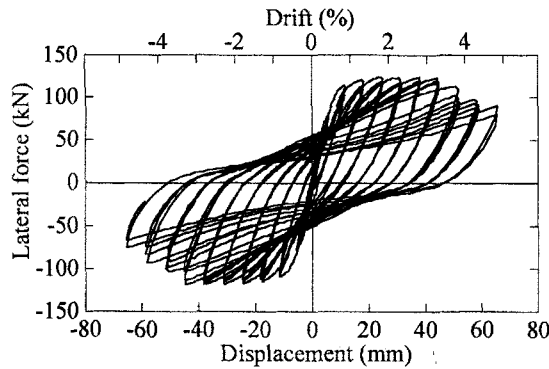


(a) Flexural hysteresis of column P1

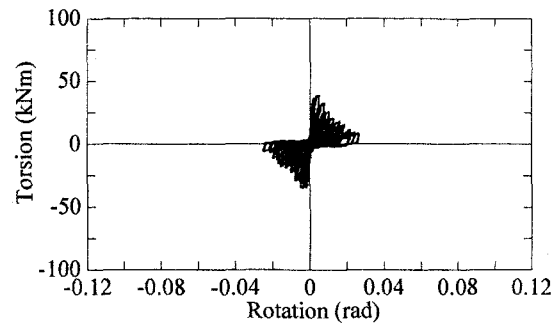


(b) Torsional hysteresis of column P3

Fig. 3 Hystereses of columns P1 under cyclic uniaxial bending and P3 under cyclic torsion

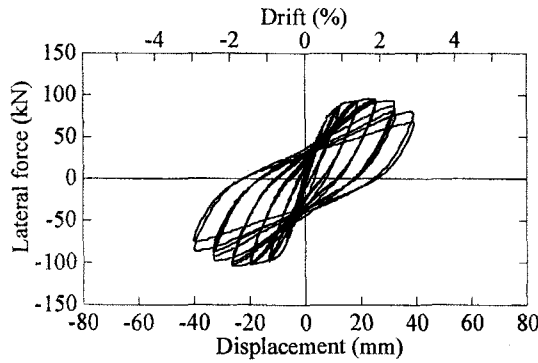


(a) Flexural hysteresis

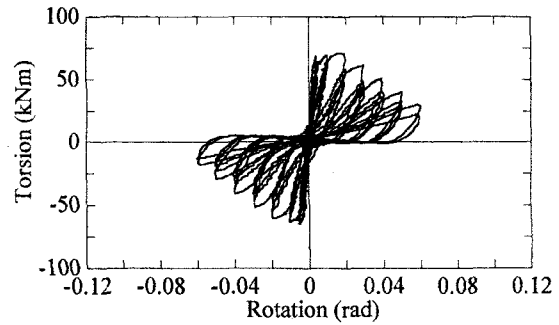


(b) Torsional hysteresis

(1) Column P4 ($r = 0.5$)



(a) Flexural hysteresis



(b) Torsional hysteresis

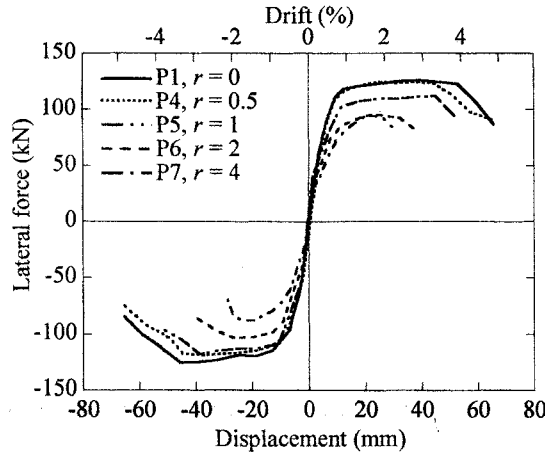
(2) Column P6 ($r = 2$)

Fig. 4 Flexural and torsional hystereses of columns P4 and P6 under combined cyclic bending and torsion

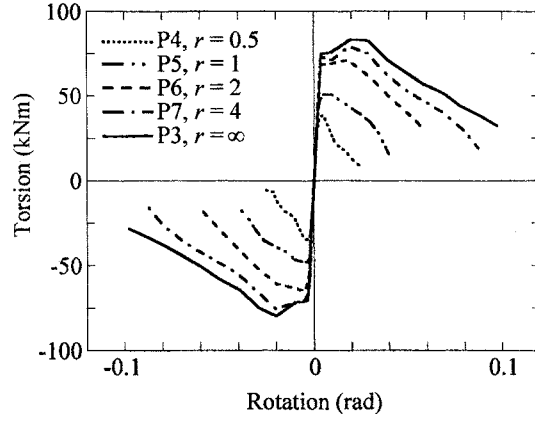
axial load, respectively. Comparing to the hystereses of P4 and P6 shown in Fig. 4, it is clearly seen that the shapes of flexural and torsional hystereses of columns under combined action are significantly different to those of P1 and P3.

The summary of flexural and torsional hysteretic envelopes is shown in Fig. 5. When the rotation-drift ratio r is small ($r = 0.5$), the flexural hysteretic envelope of a column under combined action is close to that of column under uniaxial bending. The stable lateral force zone between 1% drift to 4%

drift in P1 becomes narrower as r increases, resulted from the deterioration of initial stiffness and flexural strength and the earlier deterioration of lateral restoring force. On the other hand, in the torsional hystereses, torsion deteriorates nearly immediately after reaching a peak value as r becomes less than 1. Consequently, care has to be paid for the brittle deterioration of torsion in a column which is subjected to cyclic torsion or combined action of cyclic bending and torsion. The hysteretic envelope under combined action becomes close to that under

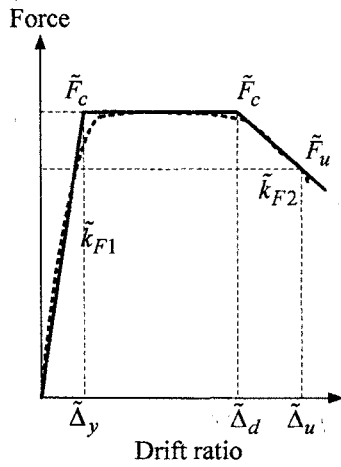


(a) Flexural hysteretic envelopes

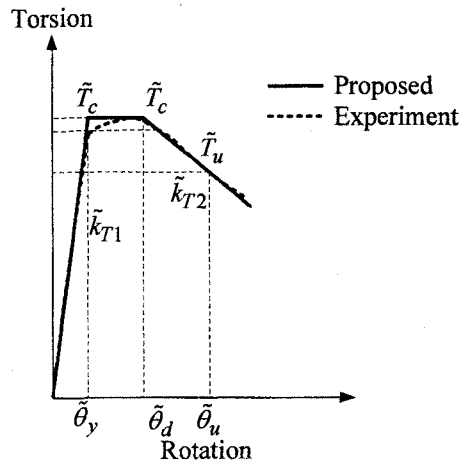


(b) Torsional hysteretic envelopes

Fig. 5 Comparison of hysteretic envelopes of columns



(a) Flexural hysteresis



(b) Torsional hysteresis

Fig. 6 Proposed hysteretic model for flexure and torsion

pure cyclic torsion as r increases.

3. PROPOSED HYSTERETIC MODEL

(1) Idealization of hysteretic model

The flexural and torsional hysteretic envelopes are idealized as shown in Fig. 6. In the flexural hysteresis, the column is assumed to be elastic with an initial flexural stiffness \tilde{k}_{F1} until the restoring force reaches the flexural strength \tilde{F}_c at the yield drift $\tilde{\Delta}_y$. This restoring force stays until column displaces to $\tilde{\Delta}_d$, and then degrades with a negative flexural stiffness \tilde{k}_{F2} to the ultimate lateral force \tilde{F}_u which is 80% of the flexural strength at $\tilde{\Delta}_u$.

The initial and deteriorating flexural stiffnesses \tilde{k}_{F1} and \tilde{k}_{F2} are defined as

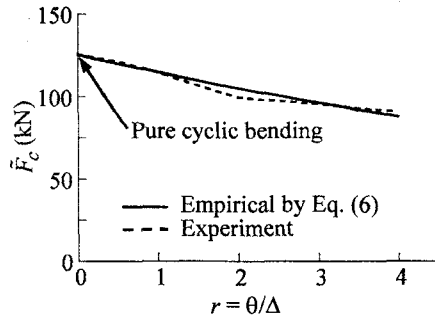
$$\tilde{k}_{F1} = \frac{\tilde{F}_c}{\tilde{\Delta}_y L_{eff}} \quad (2)$$

$$\tilde{k}_{F2} = \frac{\tilde{F}_u - \tilde{F}_c}{(\tilde{\Delta}_u - \tilde{\Delta}_d) L_{eff}} \quad (3)$$

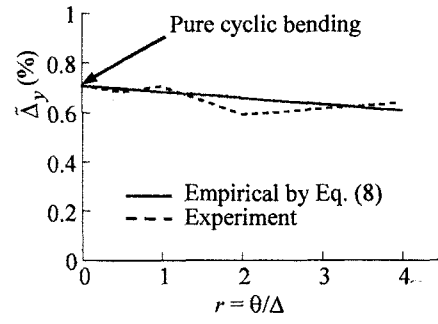
in which L_{eff} is the effective height of column.

It is noted that \tilde{k}_{F1} is obtained from the slope of a line connecting the origin and the point in which the first yield of longitudinal reinforcement occurred. $\tilde{\Delta}_d$ is obtained from the intersection between a horizontal line \tilde{F}_c and a line with a negative slope \tilde{k}_{F2} . All the above parameters are determined from the averages of the test results in the positive and negative loadings.

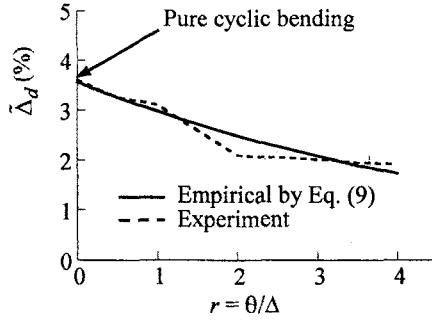
On the other hand, in the torsional hysteretic envelope, the column is assumed to behave linearly with an initial torsional stiffness \tilde{k}_{T1} until it reaches the torsional strength \tilde{T}_c at the yield rotation $\tilde{\theta}_y$. The torsion is assumed to be constant until the column rotation reaches $\tilde{\theta}_d$. The torsion deteriorates significantly over $\tilde{\theta}_d$ with a negative torsional stiffness \tilde{k}_{T2} and it is assumed that the column reaches the ultimate stage when the torsion



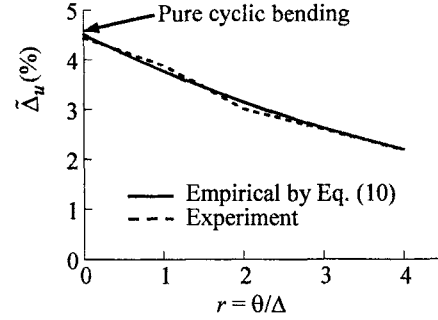
(a) Flexural strength \tilde{F}_c



(b) Yield drift $\tilde{\Delta}_y$



(c) Drift when the lateral restoring force starts to deteriorate $\tilde{\Delta}_d$



(d) Ultimate drift $\tilde{\Delta}_u$

Fig. 7 Dependence of \tilde{F}_c , $\tilde{\Delta}_y$, $\tilde{\Delta}_d$ and $\tilde{\Delta}_u$ on r

deteriorates to 80% of the torsional strength \tilde{T}_u . $\tilde{\theta}_u$ is the column rotation at ultimate.

The torsional stiffnesses \tilde{k}_{T1} and \tilde{k}_{T2} are therefore defined as

$$\tilde{k}_{T1} = \frac{\tilde{T}_c}{\tilde{\theta}_y} \quad (4)$$

$$\tilde{k}_{T2} = \frac{\tilde{T}_u - \tilde{T}_c}{\tilde{\theta}_u - \tilde{\theta}_d} \quad (5)$$

Similarly to the flexural hysteretic model, all parameters in the above torsional hysteretic model are determined from the averages of the test results in the positive and negative loadings.

(2) Effect of rotation-drift ratio on the hysteretic model

a) Flexural hysteretic model

Based on the experimental result shown in the previous section, it is obvious that the performance of the columns depends on the rotation-drift ratio r . Empirical relationships are proposed based on the regression analysis to clarify the dependency of the lateral restoring force and the displacement of a column on r .

The flexural strength of column under combined action \tilde{F}_c , which is normalized by the flexural strength of column under cyclic bending F_c ,

deteriorates as r increases as shown in Fig. 7a. This relation may be approximated as

$$\frac{\tilde{F}_c}{F_c} = e^{-0.088r} \quad (6)$$

As shown in Fig. 7a, Eq. (6) provides a good approximation with the experimental result.

Based on \tilde{F}_c by Eq. (6), the ultimate lateral restoring force \tilde{F}_u can be evaluated as

$$\tilde{F}_u = 0.8\tilde{F}_c \quad (7)$$

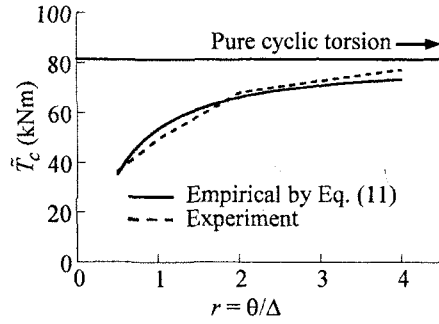
The yield drift $\tilde{\Delta}_y$, the drift when the lateral restoring force starts to deteriorate $\tilde{\Delta}_d$ and the ultimate drift $\tilde{\Delta}_u$ are likely to decrease with the increase of r as shown in Fig. 7. $\tilde{\Delta}_y$, $\tilde{\Delta}_d$ and $\tilde{\Delta}_u$ which are normalized by the yield drift of column under cyclic bending Δ_y may be approximated as

$$\frac{\tilde{\Delta}_y}{\Delta_y} = 1 - 0.035r \quad (8)$$

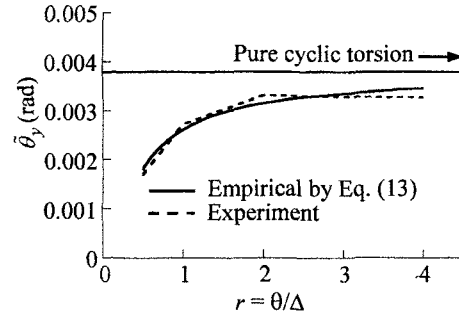
$$\frac{\tilde{\Delta}_d}{\Delta_y} = 5.03e^{-0.18r} \quad (9)$$

$$\frac{\tilde{\Delta}_u}{\Delta_y} = 6.37e^{-0.18r} \quad (10)$$

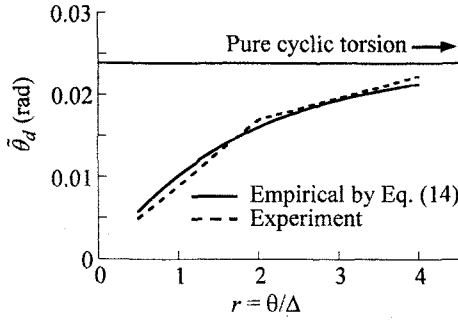
Eqs. (8) to (10) provide a good agreement with



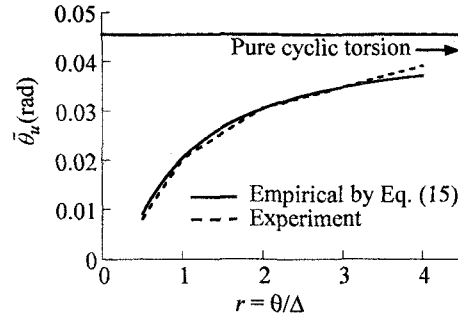
(a) Torsional strength \tilde{T}_c



(b) Yield rotation $\tilde{\theta}_y$



(c) Rotation when the torsion starts to deteriorate $\tilde{\theta}_d$



(d) Ultimate rotation $\tilde{\theta}_u$

Fig. 8 Dependence of \tilde{T}_c , $\tilde{\theta}_y$, $\tilde{\theta}_d$ and $\tilde{\theta}_u$ on r

the experimental result as shown in Fig. 7.

b) Torsional hysteretic model

In the similar way, an empirical model for torsional hysteresis is developed based on the experiment result. The torsional strength of column under combined cyclic bending and torsion \tilde{T}_c increases and approaches to the torsional strength of column under cyclic torsion T_c as r increases as shown in Fig. 8a. Therefore, \tilde{T}_c which is normalized by T_c may be approximated as

$$\frac{\tilde{T}_c}{T_c} = e^{-0.42/r} \quad (11)$$

Consequently, the ultimate torsion \tilde{T}_u can be determined from Eq. (12) as

$$\tilde{T}_u = 0.8\tilde{T}_c \quad (12)$$

The yield rotation $\tilde{\theta}_y$, the rotation when the torsion starts to deteriorate $\tilde{\theta}_d$ and the ultimate rotation $\tilde{\theta}_u$ increase and converge to the values of column under cyclic torsion as r increases as shown in Fig. 8. $\tilde{\theta}_y$, $\tilde{\theta}_d$ and $\tilde{\theta}_u$ which are normalized by the yield rotation of column under cyclic torsion θ_y may be approximated as

$$\frac{\tilde{\theta}_c}{\theta_y} = e^{-0.37/r} \quad (13)$$

$$\frac{\tilde{\theta}_d}{\theta_y} = 6.29(1 - e^{-r/1.79}) \quad (14)$$

$$\frac{\tilde{\theta}_u}{\theta_y} = 12e^{-0.8/r} \quad (15)$$

Eq. (11) and Eqs. (13) to (15) provide a good approximation with the experimental result as shown in Fig. 8.

(3) Application of proposed hysteretic model

Fig. 9 shows the correlation of the empirical hysteretic envelopes with the experiment result. The proposed empirical hysteretic model provides a good approximation to the experimental result. It should be however noted that this empirical model is developed for square columns with r ranging from 0.5 to 4. Validation of the proposed model outside this range requires further clarification.

4. CONCLUSIONS

According to the experimental result, it is obvious that the flexural and torsional strength of column decreases when the column is subjected to combined cyclic bending and torsion. Two empirical hysteretic envelopes for torsional and flexural hystereses of RC column under combined cyclic bending and torsion are proposed based on

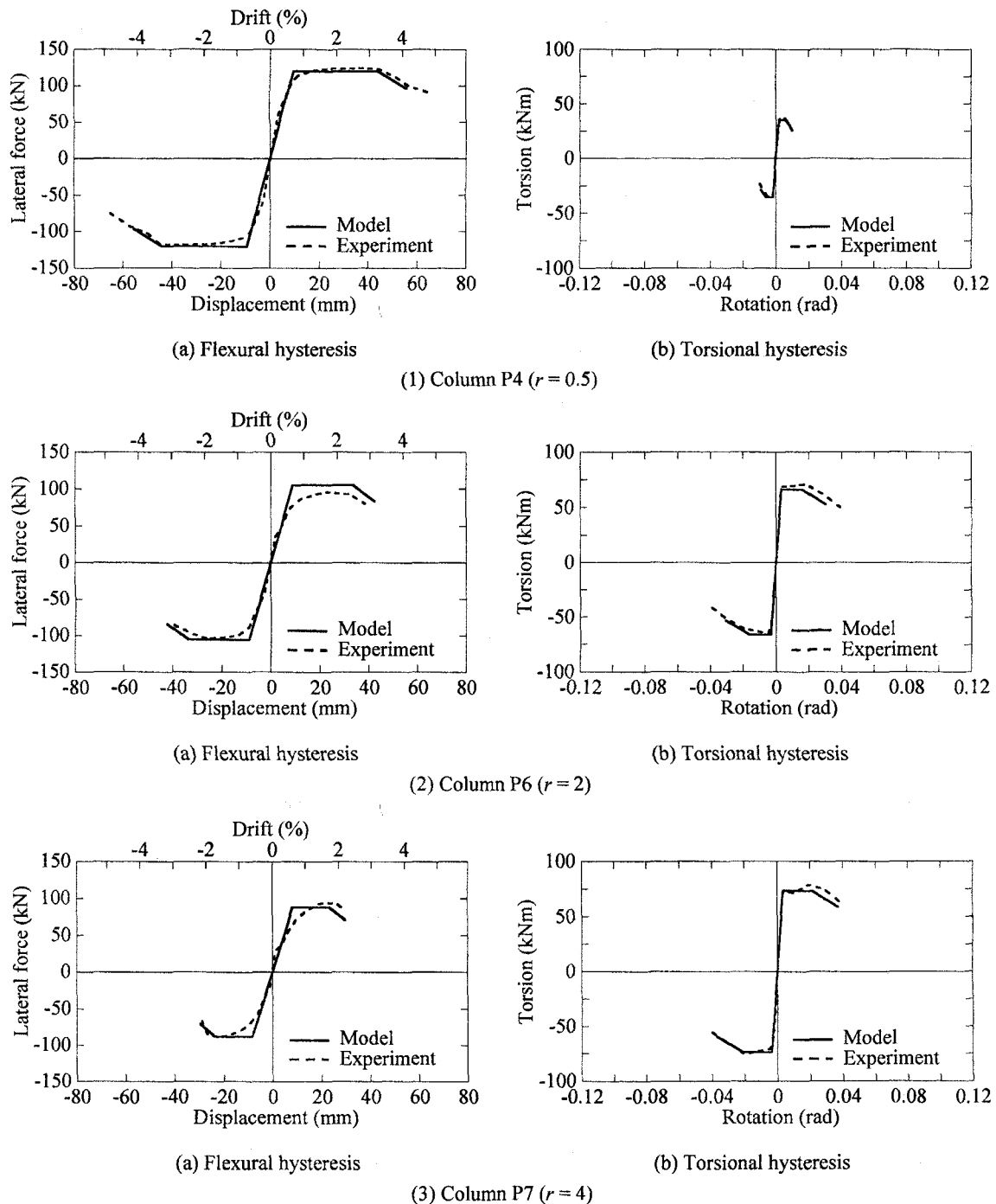


Fig. 9 Application of the proposed model to columns P4, P6 and P7 under combined cyclic bending and torsion

the experimental study to serve as the basis of the hysteretic model. They provide a good approximation to the experimental result within the range of rotation-drift ratio r between 0.5 to 4.

ACKNOWLEDGEMENT: The authors express their sincere appreciation to Messrs. Watanabe, G., Fukuda, T., Nagai, T., Wang, Y., Ogimoto, H., Kijima, K., Nagata, S., Maruyama, Y. and Ms. Sakellaraki, D. for their extensive support in constructing the columns and executing the experiment.

REFERENCES

- 1) Hsu, H.-L. and Wang, C.-L.: Flexural-Torsional Behavior of Steel Reinforced Concrete Members subjected to Repeated Loading, *Earthquake Engineering and Structural Dynamics*, Vol.29, pp. 667-682, 2000.
- 2) Hsu, H.-L. and Liang, L.-L.: Performance of Hollow Composite Members subjected to Cyclic Eccentric loading, *Earthquake Engineering and Structural Dynamics*, Vol.32, pp. 433-461, 2003.
- 3) Kawashima, K., Watanabe, G., Hatada, S. and Hayakawa, R.: Seismic Performance of C-bent Columns based on a Cyclic Loading Test, *J. of Structural Mechanics and Earthquake Engineering*, No.745/1-65, pp. 171-189, 2003. (In Japanese)

- 4) Nagata, S., Kawashima, K. and Watanabe, G.: Seismic Performance of RC C-bent Columns based on a Hybrid Loading Test, *Proc. of the 1st International Conference on Advance in Experimental Structural Engineering*, Nagoya, Japan, pp. 227-234, 2005.
- 5) Otsuka, H., Takeshita, E., Yabuki, W., Wang, Y., Yoshimura, T., and Tsunumoto, M.: Study on the Seismic Performance of Reinforced Concrete Columns subjected to Torsional Moment, Bending Moment and Axial Force, *13th World Conference on Earthquake Engineering*, Vancouver, Canada, Paper No.393, 2004.
- 6) Tirasit, P. and Kawashima, K.: Combined Cyclic Bending-Torsional Loading Test of Reinforced Concrete Bridge Columns, *21st US-Japan Bridge Engineering Workshop*, PWRI, Tsukuba, Japan, 14 pages, 2005.
- 7) Japan Road Association: *Specifications for Highway Bridges - Part V Seismic Design*, Maruzen, Tokyo, 1996.